# Highlights from the observatories

Compiled by D. J. Saikia

Interplanetary scintillation studies at Ooty

The motion of the solar-wind plasma irregularities across the line of sight modulates the intensity of radio waves seen through the inner heliosphere, giving rise to interplanetary scintillations (IPS). IPS observations can be used to infer the structure of background, compact radio sources and also study the properties of the solar wind. This has been one of the main observational programs using the Ooty Radio Telescope which operates at 327 MHz, and has yielded a number of interesting results over the years. A recent study of the turbulence spectrum of solar wind in the near-Sun region ($R<50 R_\odot$) using IPS measurements with the ORT has shown that the scintillation is dominated by density irregularities of size $\sim100-500$ km. The scintillation towards the small-scale side of the spectrum has a flatter spectrum than this dominant component, with the spectral power in the flatter portion increasing closer to the Sun. These have used to study the radial evolution of small-scale fluctuations ($\lesssim50$ km) generated by Alfvén waves (Manoharan 2010a).

IPS observations have been used to reconstruct the three-dimensional perspective views of solar co-rotating plasma and outward-flowing solar wind by iteratively fitting a kinematic solar wind model to the IPS data. This three-dimensional modeling technique permits reconstruction of the density and velocity structures of coronal mass ejections (CMEs) and other interplanetary transients. The three-dimensional reconstructions have been obtained over a 3-AU diameter heliosphere. The reconstruction of both solar wind speed and density for CME events during a highly active period, are useful to understand the heliospheric response to CMEs and co-rotating features. The reconstructions agree well with in-situ signatures observed by Wind and ACE (Advanced Composition Explorer) spacecrafts. These studies have shown that the magnetic energy possessed by the transient determines its radial evolution. A magnetically energetic CME can cause an intense geomagnetic storm, even if the trailing part of the CME passes through the Earth (Manoharan 2010b).

IPS data obtained from the ORT have been used to study the three-dimensional evolution of density turbulence in the heliosphere over the period 1995−2010. The large-scale features of solar wind speed and density turbulence during the minimum phase of solar cycle No. 23 are
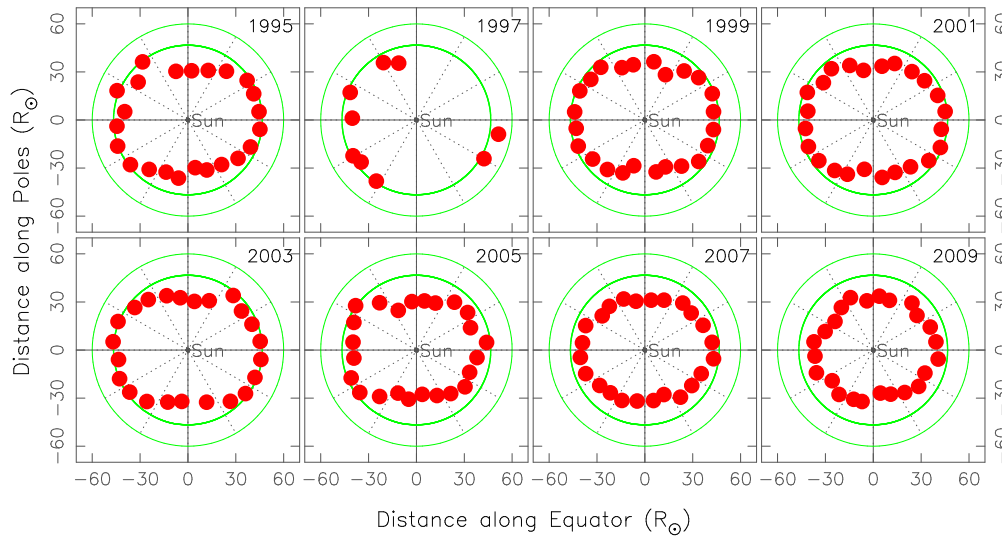
Figure 1. Shape of constant density turbulence contours around the Sun during years 1995 to 2009. In these plots, the Sun is at the centre and X and Y axes represent, respectively, heliocentric distances along the solar equator and poles. During the last solar minimum, after about year 2003, the density contours steadily shrunk close to the Sun, indicating a gradual decrease in the scattering diameter of the corona (Manoharan 2010c).

remarkably different from that of the previous cycle. The results on solar wind density turbulence show that (i) the current solar minimum is experiencing a low level of coronal density turbulence, (ii) the scattering diameter of the corona has decreased steadily starting from 2003, i.e., during the declining phase of the activity, and (iii) the turbulence at a given distance in the heliosphere, irrespective of latitude, has remained nearly at the same level between 1989 and 2003, but decreased steadily after 2003 (Fig. 1). These are likely related to weak solar magnetic fields, with the implication that the supply of mass and energy from the Sun to the interplanetary space has significantly reduced in the present low level of activity (Manoharan 2010c).

Optical polarimetry and photometry of comet 17P/Holmes and 67P/Churyumov-Gerasimenko

Polarization observations of comets have proved to be an important tool to study the physical properties of cometary dust. The polarization is caused by the scattering of solar radiation by the cometary dust, with the degree of polarization and its orientation depending on the size and composition of the dust particles, the phase angle and the wavelength of the incident radiation.

Comet 17P/Holmes which exhibited a spectacular outburst on 2007 October 24, five months after perihelion passage, was observed for linear polarization using the optical polarimeter mounted

at the 1.2m telescope at Mt. Abu Observatory, during 2007 November 5−7 and then on 2007 December 13 by Joshi, Ganesh & Baliyan (2010). Observations were conducted through the International Halley Watch (IHW) narrow-band (continuum) filters. During the observing run the phase angle was near 13°. Joshi, Ganesh & Baliyan report the polarization values to be ∼−1.5 per cent; the negative polarization at low phase being consistent with polarization values of other typical comets. They find that the coma shows an increase in relative abundance of smaller dust particles away from the nucleus (Joshi, Ganesh & Baliyan 2010).

Imaging polarimetric observations were conducted at the Haute-Provence observatory on 2009 March 17−19 at 35° phase angle and at IUCAA Girawali observatory (IGO) on 2008 December 25−27 at 36° phase angle and on 2009 April 30−May 1 at 29° phase angle (Hadamcik et al. 2010). The authors suggest the presence of rather large particles before and just after perihelion and the ejection of post-perihelion smaller grains, eventually in fluffy aggregates. A strong seasonal effect related to the obliquity of the comet suggests that the different grains originate in different hemispheres of the nucleus (Hadamcik et al. 2010).

An ingress and a complete transit of HD 80606 b

The hot Jupiters, which are about the mass of Jupiter or larger, and orbit about a fraction of an astronomical unit from their host stars, form an important class of extra-solar planets. These planets are likely to be significantly affected by radiation and tidal forces from the parent star and could provide interesting constraints on the physical properties of planetary atmospheres (cf. Irwin et al. 2008). Naef et al. (2001) reported the discovery of a planet, HD 80606 b, in a 111-d orbit around the star HD 80606. Its mass is at least 3.9 times the mass of Jupiter and has the most eccentric orbit (e=0.93) of all extra-solar planets. The IGO was used along with three other telescopes to obtain near-continuous light-curve coverage of the star as it was transited by the planet during the predicted transit windows around 2008 October 25 and 2009 February 14. From this unique data set, they find system parameters consistent with earlier estimates, but a slightly smaller planet-to-star radius ratio corresponding to a planet radius of $0.921 \pm 0.036 R_{Jup}$ (Hidas et al. 2010).

Carbon stars

Polarization observations provide interesting information on physical conditions in the stellar environment during different stages of stellar evolution. For example, stars with circumstellar material exhibit linear polarization with the degree of polarization increasing with asymmetries in the geometry of the shells. Also, for stars evolving from a red giant to a planetary nebula, the observed polarization reaches a maximum during the proto-planetary stage and decreases as the star evolves into a planetary nebula (e.g. Johnson & Jones 1991).

Aruna Goswami, Sreeja Kartha and Asoke Sen have reported the first-ever estimates of *V*-band polarimetry of a group of CEMP (carbon-enhanced metal-poor) stars using the IGO. Al-

though their sample size is small, they find that the stars separate into two distinct groups, ones with the degree of polarization, p<0.4 per cent, while the others are with p>1 per cent. Extending this study to a larger sample of sources, and examining its time variability as well as radial velocity variations and binary nature of these stars should help understand the differences (Goswami, Kartha & Sen 2010).

Aruna Goswami and her collaborators continued their spectroscopic search for CH stars from the Hamburg/ESO Faint High Latitude Carbon Stars survey. CH stars form a distinct type of carbon star which has strong molecular bands of CH. Their characteristic properties such as iron deficiency, enrichment of carbon and overabundance of heavy elements help in providing observational constraints for models of nucleosynthesis at low metallicity. Goswami, Karinkuzhi & Shantikumar (2010a) used both the 2.3 m Vainu Bappu Telescope and the 2 m Himalayan Chandra Telescope (HCT) and found that 36 of 92 candidates observed are potential CH stars. The total number of stars observed by the group has now reached 243. During this survey, they discovered a hydrogen deficient CH star at high galactic latitude using the Himalaya Faint Object Spectrograph (HFOSC) on HCT. This star HE 1015−2050 adds to a rare class of which 51 members are known in our Galaxy, 15 in the LMC and 5 in the SMC (Goswami, Karinkuzhi & Shantikumar 2010b).

Towards an empirical theory of pulsar emission

The characteristics of radio pulsar profiles have been studied over the years in order to understand their emission processes. Detailed studies of profiles have led to the identification of two distinct components, the core and conal components, which are related to the magnetic field lines in the vicinity of the pulsars. The core emission arises from a narrow beam close to the stellar surface, while the conal emission forms a conical beam above the stellar surface. The common triple (T) profile consists of a core and is preceded and followed by conal components, while a double-conal pulsar could be a five-component (M) one (Rankin 1993, and references therein for a detailed discussion).

Dipanjan Mitra and Joanna Rankin have studied a group of pulsars which were classified by Lyne & Manchester (1988) as ones with 'partial cones' which were characterized by their asymmetric average profiles and asymmetric polarization position angle (PPA) traverses, and difficult to interpret in the standard core/cone scenario. From single-pulse, very sensitive polarimetric observations of these pulsars with the Giant Metrewave Radio Telescope (GMRT) and the Arecibo Observatory, they find that most of these 'partial cones' exhibit a core/cone structure just as the normal pulsars, although the emission above different areas of their polar caps can be very asymmetric. Effects of aberration and retardation could play a significant role in distorting the core/cone emission-beam structure in rapidly rotating pulsars (Mitra & Rankin 2011).

Lunar occultation of sources in the near-infrared towards the Galactic Centre

Lunar occultation observations in the infrared could provide information on source structures with angular resolutions of a few milliarcsec towards regions which are heavily obscured at optical wavelengths. During one of the relatively rare passages of the moon in the direction of the high stellar density regions of the Galactic Centre, Chandrasekhar & Baug (2010) observed a dozen events in the K band using the fast subarray mode of operation of the NICMOS IR camera attached to the 1.2 telescope at Mt Abu. While a majority of the sources appear unresolved (<3 milliarcsec), three sources are clearly resolved and have uniform disk angular sizes ranging from 7 to 18 milliarcsec. Two of these sources are late M giants while one is a carbon star. In addition, one is a possible binary system with a projected separation of 30±5 milliarcsec (Chandrasekhar & Baug 2010).

Binary systems

Aviles et al. (2010) used multisite photometric data that included HCT amongst 5 telescopes distributed between Korea and Mexico to derive the photometric period of the cataclysmic binary SDSS J123813.73−033933.0. Using infrared photometry from 6.5 m Baade/Magellan telescope, and optical spectroscopy with 2.1 m telescope at San Pedro Martyr, Mexico, they conclude that the system comprises of a massive white dwarf of temperature 12000 K and a brown dwarf of type L4.

The W UMa type contact binary EK Comae Berenices and the newly discovered contact binary ASAS 134738+0410.1 were observed photometrically with the 2-m telescope of IGO, and the elements of the binaries were determined (Deb et al. 2010a,b).

Near infrared studies of the 2010 outburst of the recurrent nova U Scorpii

Novae which undergo multiple outbursts are known as recurrent novae (RNe). These outbursts occur due to thermonuclear runaway on the surface of a white dwarf due to accretion of mass from a companion star (e.g. Kato 1990). The outburst mechanism is identical to that of classical novae, but the presence of a high-mass WD (mass greater than about $1.3M_\odot$) and a high accretion rate cause the short recurrence timescale. RNe, of which only 10 are known in our Galaxy, are special because they are strong progenitor candidates of Type Ia supernovae, objects of cosmological importance. The well-known recurrent nova U Scorpii underwent its most recent eruption in 2010, which was studied in an extensive global effort across all wavelengths. The present eruption was preceded by at least six previous observed outbursts between 1863 and 1999. Dipankar P.K. Banerjee and his collaborators obtained the IR light curve and recorded several spectra, starting as early as 0.59 days after outburst, to study the the IR evolution of the nova. The mass of the ejecta was determined from Case B recombination analysis. The highlight of the spectra is the presence
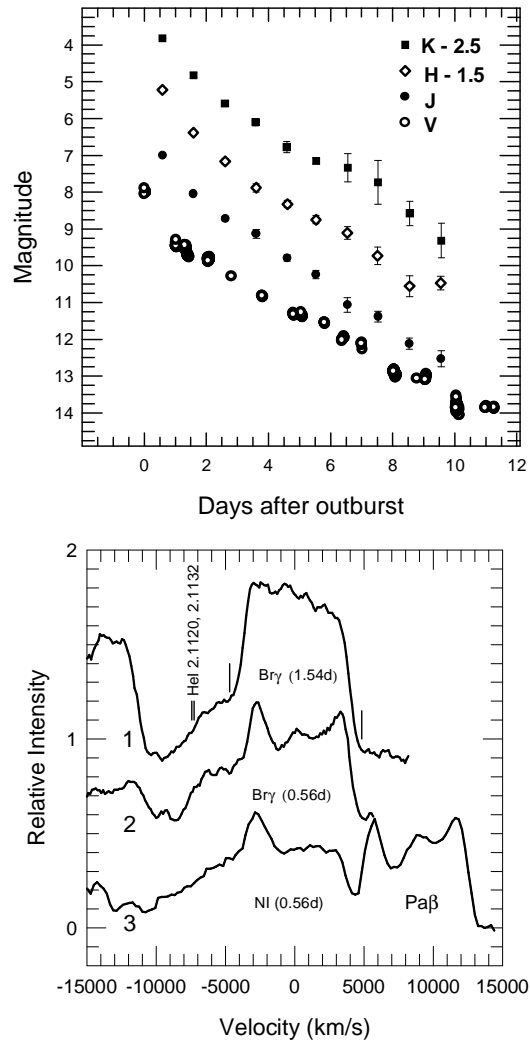
Figure 2. Top panel:The near-IR and visual light curve of U Sco during the early decline phase. The V-band data are from AAVSO. The J, H, K magnitudes have been offset as indicated for clarity. Bottom panel: Velocity profiles 1 and 2 are for Brγ on days 1.54 and 0.56, respectively; they have a core component between -4700 and $+4850$ km s^{-1} (marked by lines), and an extended blue wing. The expected positions of He$\scriptstyle\rm I$ 2.1120, 2.1132 μm lines are shown. Profile 3 is for the N$\scriptstyle\rm I$ 1.2461, 1.2470 μm line on day 0.56, which also shows an extended blue wing. The ordinate is in arbitrary units with the profiles offset for clarity. Both the figures have been reproduced from Banerjee et al. (2010).

of very broad wings in several spectral lines, with tails extending up to 10,000 km s^{-1} along the line of sight - the true velocities could hence be considerably larger (Fig. 2). It is unexpected for a nova to exhibit ejection velocities similar to those usually thought to be exclusive to supernovae (Banerjee et al. 2010).

Open and globular clusters

An important issue in our understanding of masive star formation is the sequence of formation of low- and high-mass stars in a cluster environment (e.g. Zinnecker & Beuther 2008). Devendra Ojha and his collaborators have studied star formation in the young stellar cluster IRAS 19343+2026 using optical observations from HCT and infrared observations from the United Kingdom Infrared Telescope (UKIRT). They detected young, massive stars of age $<10^5$ yr along with an older (1−3 Myr) population of low-mass young stellar objects (YSOs). They propose a scenario of lower mass stars forming prior to the higher mass stars. The total mass of the cluster is in the range of ∼300−600 M$_\odot$, and the initial mass function appears to be shallower than Salpeter's mass function (Ojha et al. 2010).

Mathew, Subramaniam & Bhavya (2010) used optical imaging and spectroscopy with the HCT supplemented by Two Micron All Sky Survey (2MASS) infrared data to study Herbig Ae/Be stars in four young open clusters. These stars were identified by them as emission line stars based on an earlier survey with the HCT. All the stars exhibit near-infrared excess. The ages of these stars were found to be in the range of 0.25−3 Myr. They also present evidence for continuous star formation in these clusters over the last 10 Myr.

Subramaniam, Carraro & Janes (2010) observed 10 unstudied open clusters using BVI CCD photometry with the HCT and estimated their fundamental parameters. For eight of these clusters, the photometry was conducted for the first time. Six of these clusters are well above or below the Galactic plane. Seven clusters have ages <500 Myr, but three are older than 1 Gyr. Eight of these are beyond a distance of 2 kpc distance. The study has significantly increased the number of well-studied clusters at such distances in the second half of the first Galactic quadrant.

Arellano Ferro, Giridhar & Bramich (2010) studied the RR Lyrae, Blue Stragglers and SX Phoenicis stars in the globular cluster NGC 5053 through photometric monitoring. They improved the periods and reported new times of maximum light for eight RR Lyrae stars, new periods for 5 SX Phoenicis stars, and the discovery of new Blue Stragglers. They also estimated the iron abundance, masses and radii of stars in the cluster, and obtained a distance of 16.7±0.3 kpc for the cluster and 12.5±2.0 Gyr for its age.

Galactic star forming regions

Samal et al. (2010) investigated the morphology, physical-environment, stellar content and star formation activity in the vicinity of star-forming region Sh 2-100 and found that the region con-
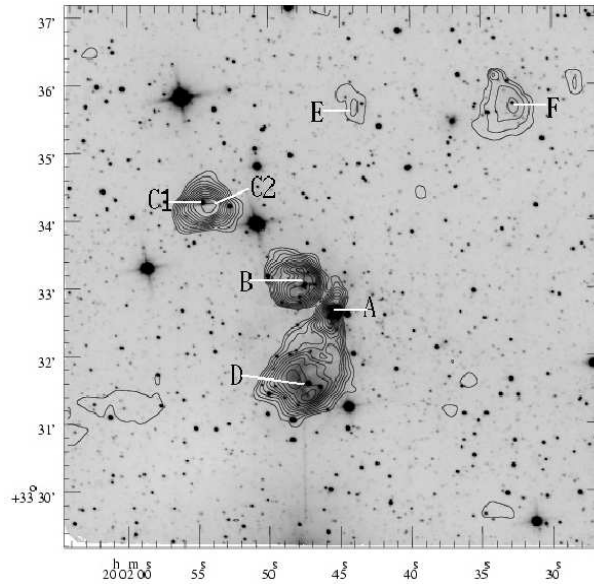
Figure 3. IRSF K$_s$-band image in logarithmic scale overlaid with the GMRT radio continuum contours at 610 MHz. Individual H$_{II}$ regions are marked in the Figure which is reproduced from Samal et al. (2010).

tains seven H$_{II}$ regions of ultracompact and compact nature, all belonging to the same molecular cloud complex (Fig. 3). Multiwavelength data obtained using the Sampurnanand telescope of ARIES (photometry), HCT (optical imaging and spectroscopy), Infrared Survey Facility (IRSF) for near-infrared imaging, and GMRT (radio continuum), were supplemented by archival infrared data from 2MASS, Spitzer, Midcourse Space Experiment (MSX) and Infrared Astronomical Satellite (IRAS). The most probable ionizing sources of six H$_{II}$ regions were identified with OB stars. The morphology of the complex shows a non-uniform distribution of warm and hot dust, well mixed with the ionized gas, which correlates well with the variation of average visual extinction (4-97 mag) across the region. The H$_{II}$ regions were found to be in different stages of evolution, depending on the age of the ionizing sources which are in the range of 0.01−2 Myr. It appears that star formation in Sh 2-100 region is induced by an expanding H$_I$ shell (Samal et al. 2010).

The transient source GCRT J1745−3009

GCRT J1745−3009 is an interesting radio-selected transient source which when active emits bursts with a peak flux density ∼1 Jy which lasts ∼10 min and repeats itself every 77 min (Hyman et al. 2007, and references therein). Subhashis Roy and his collaborators have reported the detection of strong circularly polarized emission from GCRT J1745−3009 based on new analysis of 325 MHz GMRT observations conducted on 2003 September 28. They place 8R$_\odot$ as the upper
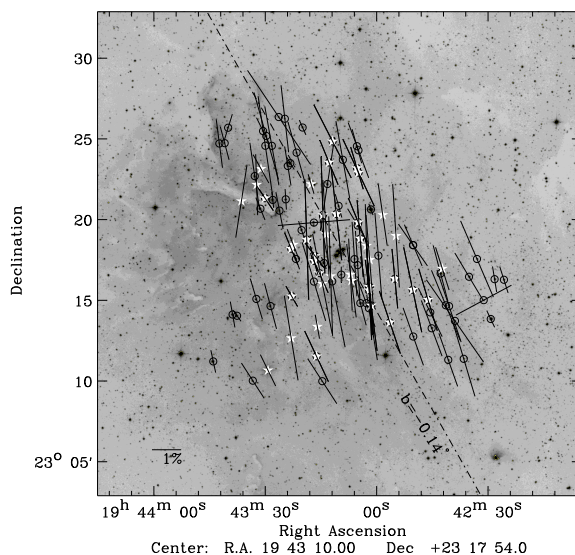
Figure 4. The 30×30 arcmin² R-band DSS2 image of the field containing NGC 6823 with the polarization vectors drawn with the star as the centre. The length of the polarization vectors is proportional to the percentage of polarization, and is oriented parallel to the direction corresponding to the observed polarization position angle. Polarization vectors of 12 stars observed by Serkowski (1965) are shown in white. The figure is reproduced from Medhi et al. (2010).

limit on the size of the emission region, firmly establishing that the emission is coherent. Electron cyclotron or plasma emission from a highly subsolar magnetically dominated dwarf located $\lesssim 4$ kpc away could have given rise to the GCRT radio emission (Roy et al. 2010).

Polarization observations towards open clusters

The polarization of starlight caused by asymmetric dust grains which are partially aligned by the interstellar magnetic field has been an important tool to study the magnetic field and also physical properties of interstellar dust. Polarimetric studies of open clusters can provide valuable information on foreground interstellar dust, since the distance, membership probability and colour excess of the stars are available. The ARIES Imaging Polarimeter (AIMPOL; Medhi et al. 2007) mounted on the Cassegrain focus of the 104-cm Sampurnanand Telescope of ARIES, Nainital, has been used to study several open clusters, with detailed results being reported recently for NGC1893 (Eswaraiah et al. 2011) and NGC6823 (Medhi et al. 2010).

Multiwavelength linear polarimetric observations for 44 stars of the NGC 1893 young open

cluster region along with V-band polarimetric observations of stars of four other open clusters located between l ~160° and 175° have been reported by Eswaraiah et al. (2011). They find evidence for the presence of two dust layers located at a distance of ~170 and ~360 pc. The dust layers produce a polarization of ~2.2 per cent, and in this region of the Galactic plane, the polarization angles remain almost constant, with a mean of ~163° and a dispersion of 6° (Eswaraiah et al. 2011). Multiwavelength linear polarimetric observations of 104 stars towards the region of young open cluster NGC 6823 (Fig. 4), have shown evidence for the presence of several layers of dust towards the line of sight (Medhi et al. 2010). The first layer of dust is approximately located within ~200 pc, which is much closer to the Sun than the cluster itself (~2.1 kpc). The distribution of the foreground dust grains is patchy, leading to differential reddening and polarization towards NGC6823 (Medhi et al. 2010).

Hɪ opacity fluctuations towards Cassiopeia A

Hɪ 21cm opacity fluctuations in our Galaxy have been reported on scales ranging from as small as ~5 to 3000 AU (Brogan et al. 2005; Frail et al. 1994; Hennebelle & Audit 2007, and references therein), although their origin and physical properties are not well understood. Nirupam Roy and his collaborators have presented the Hɪ 21cm opacity fluctuations power spectrum towards the supernova remnant Cas A from GMRT observations with a spatial resolution of 5 arcsec and spectral resolution of 0.4 km s^{-1}. They find that the power spectrum is well fitted by a power law with an index of -2.86 ± 0.10 over scales of $0.07-2.3$ pc for gas in the Perseus arm and over 0.002-0.07 pc in the local arm (Roy et al. 2010).

Short-period Cepheids in the disk of M31

Although the main aim of the Nainital Microlensing Survey using the 1-m Sampurnanand Telescope was to search for micolensing events in the direction of M31, the data have been used to identify short-period and relatively faint Cepheids in the disk of M31. Cepheids are the primary distance indicators and they are important for determining precise distances as well as for understanding the star formation history of the galaxy. Joshi et al. (2010) present a catalogue of 39 short-period (P<15 days) Cepheids in ~13×13 arcmin^2 region of the M31 disk, with periods as short as ~3.4 days.

Thick gas discs in faint dwarf galaxies

Sambit Roychowdhury and his collaborators have determined the the intrinsic axial ratio distribution of the gas discs of extremely faint $M_B >-14.5$ dwarf irregular galaxies, using those observed as part of the Faint Irregular Galaxy GMRT Survey (FIGGS; Begum et al. 2008). They find that the Hɪ discs of faint dwarf irregulars are quite thick, with mean axial ratio of ~0.6, substantially larger than the typical value of ~0.2 for the stellar discs of large spiral galaxies. They note that

this is consistent with the much larger ratio of velocity dispersion to rotational velocity in dwarf galaxy HI discs compared with those in spiral galaxies (Roychowdhury et al. 2010).

GMRT observations of HI absorption in quasar-galaxy pairs

HI 21-cm absorption observations have proved to be an important tool for probing HI gas at moderate and higher redshifts, where emission line gas is often below the current detection thresholds. Detection of 21-cm absorption depends on the strength of the background radio source and 21-cm absorption cross-section of the foreground absorber. Neeraj Gupta and his collaborators have presented the results of a small GMRT survey of 21-cm absorption of five quasar-galaxy pairs with the redshifts of the galaxies in the range $0.03 \leq z_g \leq 0.18$, selected from the Sloan Digital Sky Survey (SDSS). The HI 21-cm absorption was searched towards the nine sightlines with impact parameters ranging from ~10 to 55 kpc, and detected towards one pair with an impact parameter of ~11 kpc. In the remaining cases, the upper limits on N(HI) are in the range (10^{17} to 10^{18}) T_s cm^{-2}. Combining data from the literature they explore the possibility that the current sample of damped Lyα absorbers may be a biased population avoiding sight lines through dusty star-forming galaxies (Gupta et al. 2010).

Clusters of galaxies

Diffuse, low-surface brightness radio sources observed in the central regions of massive galaxy clusters, and which appear extended on Mpc scales but are not associated with individual galaxies are referred to as radio halos. Macario et al. (2010) present a detailed GMRT study of the giant radio halo in the galaxy cluster Abell 697. Their sensitive 325-MHz image shows the halo to be bigger than earlier observations (Fig. 5), and its spectral index to be very steep ($\alpha \sim 1.7-1.8$, where $S \propto \nu^{-\alpha}$). They do not prefer a hadronic origin and suggest that turbulence could be playing a significant role (Macario et al. 2010).

Ruta Kale and Dwarakanath have imaged Abell 2256 at 150 MHz and detected the diffuse radio halo and relic emission over an extent of ~1.2 Mpc. They determined the spectral index distributions using the GMRT image and archival observations from the Very Large Array (VLA; 1369 MHz) and the Westerbrok Synthesis Radio Telescope (WSRT; 330 MHz). These spectral indices indicate synchrotron lifetimes for the relativistic plasmas in the range 0.08−0.4 Gyr. Their study also suggests that the spectra could be due to two populations of relativistic electrons created at two different epochs due to mergers (Kale & Dwarakanath 2010).

Macario et al. (2011) have presented new Chandra X-ray and GMRT radio observations of the nearby merging galaxy cluster Abell 754. Their X-ray data confirm the presence of a shock front while their GMRT observations at 330 MHz show that the centrally located radio halo extends eastward to the position of the shock. The X-ray shock front also coincides with the position of a radio relic previously observed at 74 MHz. They find the radio spectrum of the

post-shock region to be very steep, and suggest that the acceleration of electrons at the shock front is possibly due to reacceleration of pre-existing relativistic electrons (Macario et al. 2011).
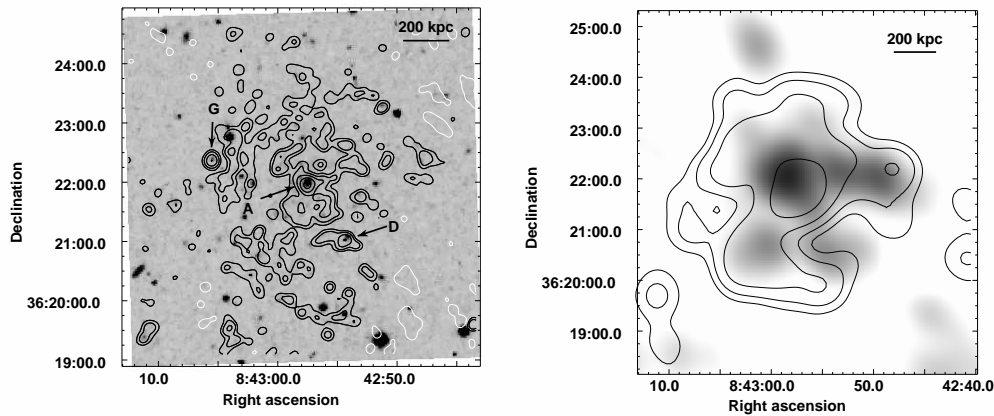
Figure 5. Left panel: Full-resolution (∼10 arcsec) GMRT 325 MHz contours of the central region of Abell 697, superposed to the Second Palomar Sky Survey (POSS-2) optical image. The individual radio sources are labelled. Right panel: Low-resolution (∼45 arcsec) image of the radio halo at 325 MHz after subtracting the individual sources overlaid on the GMRT 610 MHz image (grey scale). Figure reproduced from Macario et al. (2010).

Comparison of radio and X-ray images have continued to provide interesting information in our understanding of cooling flows in clusters of galaxies and the effects of an active galactic nucleus on the intracluster gas. Gitti et al. (2010) report the results of an analysis of Chandra, XMM-Newton, and new GMRT data of the X-ray bright compact group of galaxies HCG 62, which is one of the few groups known to possess clear, small X-ray cavities in the inner regions. While the HCG 62 cavity system shows minimal if any radio emission at high frequencies, the new GMRT observations at 235 MHz and 610 MHz clearly detect extended low-frequency emission from radio lobes corresponding to the cavities. They find evidence of a shock front and suggest that the the radio source is radiatively inefficient, and that the radio pressure of the lobes is about 1 order of magnitude lower than the X-ray pressure of the surrounding thermal gas (Gitti et al. 2010).

Murgia et al. (2010) have observed the radio mini-halo surrounding a faint compact radio source in the Ophiuchus cluster of galaxies at low frequencies using the GMRT, and studied the spectral index of the minihalo. The minihalo has a spectral index of ∼1.60±0.05 between 240 and 1477 MHz and also shows evidence of steepening with radius. They estimate that the electron energy spectrum should extend from a minimum Lorentz factor of ≲700 to a maximum value of

3.8×10^4 with an index of 3.8±0.4, and the volume-averaged strength for a completely disordered intra-cluster magnetic field is 0.3±0.1 μG (Murgia et al. 2010).

Nirupam Roy, Chandreyee Sengupta, and Nimish Kantharia have identified an interesting group of galaxies at a redshift of 0.069. J113924.74+164144.0 exhibits tidal-tail-like extended optical features on both sides, and has a neighbouring spiral galaxy which has a strikingly similar tidal morphology and a fainter galaxy. They find the HI emission from the galaxy to be extended and significantly offset from the optical position of the galaxy, possibly due to interactions with the neighbouring spiral galaxy. They also detect HI from another spiral at a projected distance of 600 kpc, suggesting that they form a loose group at z=0.069 (Roy, Sengupta & Kantharia 2010).

Radio galaxies and quasars

High-redshift radio galaxies (HzRGs), at redshifts $\gtrsim 2$, are useful probes of the high-redshift Universe and also for constraining models and physical properties of radio galaxies (see Miley & de Breuck 2008). Many of these high-redshift galaxies have been identified from very steep-spectrum radio sources. Keeping this in mind, Ishwara-Chandra and collaborators are attempting to identify HzRGs which are 10 to 100 times deeper than the known ones from deep GMRT observations of selected fields. They present their results on 150-MHz observations of the LBDS-Lynx field (Fig. 6). Their image has an rms noise of ~0.7 mJy beam^{-1} and is the deepest low-frequency image of this field. They have combined their results with existing WSRT and VLA observations to identify 150 radio sources with a spectral index steeper than 1. Many of these are not detected in the Sloan Digital Sky Survey and are candidate HzRGs (Ishwara-Chandra et al. 2010).

Sumana Nandi and her collaborators have presented low-frequency observations with the GMRT starting from 150 MHz and high-frequency observations with the VLA to estimate the spectral ages and examine any evidence of diffuse extended emission at low radio frequencies due to an earlier cycle of activity (see Saikia & Jamrozy 2009 for a review) in two large radio galaxies 3C46 and 3C452. While no evidence of extended emission due to an earlier cycle of activity has been found, their spectral ages have been estimated to be ~15 and 27 Myr for the oldest relativistic plasma respectively. The spectra in the vicinity of the hotspots are consistent with a straight spectrum with injection spectral indices of ~1.0 and 0.78, respectively, somewhat steeper than theoretical expectations (Nandi et al. 2010).

GMRT Epoch of Reionization experiment

The Epoch of Reionization (EoR) represents the period in the history of our Universe when the predominantly neutral hydrogen gas was ionized by the emergence of the first stars, galaxies or quasars. After the recombination epoch at z ~1100, the Universe was filled with neutral hydrogen till it was locally ionized by these luminous objects. This was the start of the EoR. With time the ionized regions grew, creating a network of ionized and neutral regions. Studies of reionization can provide valuable information on structure formation in the Universe.
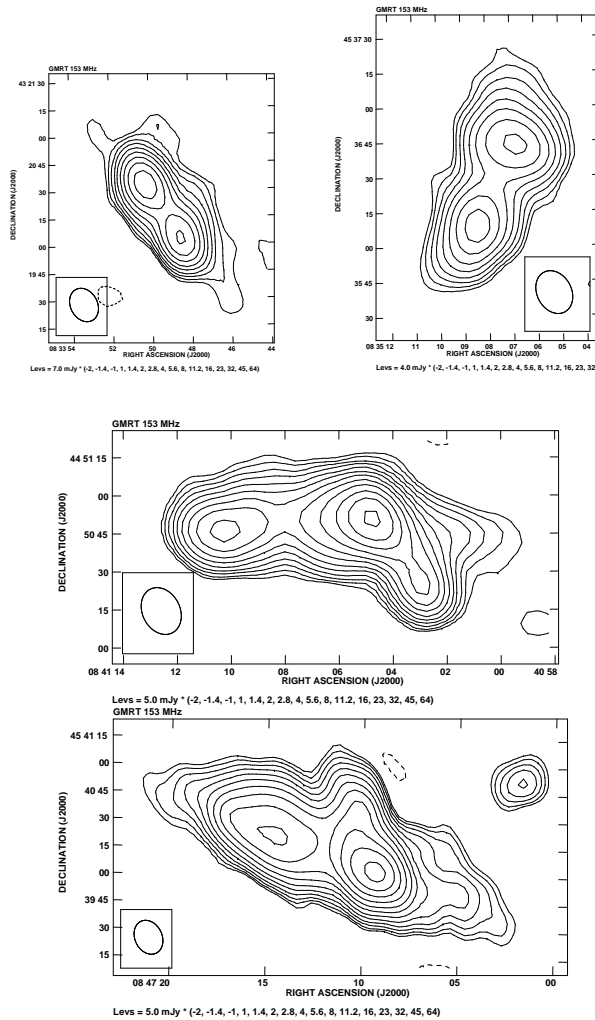
Figure 6. A few of the extended steep-spectrum sources imaged at 150 MHz with the GMRT in the LBDS-Lynx field (Ishwara-Chandra et al. 2010).

Paciga et al. (2011) have made GMRT observations near 150 MHz to measured the power spectrum of 21-cm brightness temperature fluctuations, and have set a new upper limit on brightness temperature fluctuations at $z \sim 8.6$. This required careful removal of radio frequency interference (RFI) and foreground subtraction. Their upper limit of approximately 70 mK on the variance in 21-cm brightness temperature at z=8.6 is almost two orders of magnitude better than previous limits (Paciga et al. 2011).

A real-time software backend for the GMRT

Software signal processing is having a significant impact on radio astronomy instrumentation. Jayanta Roy and his collaborators have reported recently their design and implementation of a 33 MHz bandwidth, 32 station, dual polarization, fully real-time software backend system for the GMRT, using off-the-shelf components. They have built a correlator and a beamformer, using PCI-based ADC cards and a Linux cluster of 48 nodes with dual gigabit inter-node connectivity for real-time data transfer requirements. Their approach has allowed a relatively rapid development of a fairly sophisticated and flexible backend receiver system, which will greatly enhance the productivity of the GMRT. They have successfully validated the backend and has released it for regular use (Roy et al. 2010).

Acknowledgments

References

Arellano Ferro A., Giridhar S., Bramich D.M., 2010, MNRAS, 402, 226

Aviles A., et al., 2010, ApJ, 711, 389

Banerjee D.P.K., et al., 2010, MNRAS, 408, L71

Begum A., Chengalur J.N., Karachentsev I.D., Sharina M.E., Kaisin S.S., 2008, MNRAS, 386, 1667

Brogan C.L., Zauderer B.A., Lazio T.J., Goss W.M., DePree C.G., Faison M.D., 2005, AJ, 130, 698

Chandrasekhar T., Baug T., 2010, MNRAS, 408, 1006

Deb S., Singh H.P., Seshadri T.R., Gupta R., 2010a, BASI, 38, 77

Deb S., Singh H.P., Seshadri T.R., Gupta R., 2010b, New Astr., 15, 662

Eswaraiah C., Pandey A.K., Maheswar G., Medhi B.J., Pandey J.C., Ojha D.K., Chen W.P., 2011, MNRAS, 411, 1418 (arXiv:1009.5578)

Frail D.A., Weisberg J.M., Cordes J.M., Mathers C., 1994, ApJ, 436, 144

Gitti M., O'Sullivan E., Giacintucci S., David L.P., Vrtilek J., Raychaudhury S., Nulsen P.E.J., 2010, ApJ, 714, 758

Goswami A., Kartha S.S., Sen A.K., 2010, ApJ, 722, L90

Goswami A., Karinkuzhi D., Shantikumar N.S., 2010a, MNRAS, 402, 1111

Goswami A., Karinkuzhi D., Shantikumar N.S., 2010b, ApJ, 723, L238

Gupta N., Srianand R., Bowen D.V., York D.G., Wadadekar Y., 2010, MNRAS, 408, 849

Hadamcik E., Sen A.K., Levasseur-Regourd A.C., Gupta R., Lasue J., 2010, A&A, 517A, 86

Hennebelle P., Audit E., 2007, A&A, 465, 431

Hidas M.G., 2010, MNRAS, 406, 1146

Hyman S.D., Roy S., Pal S., Lazio T.J.W., Ray P.S., Kassim N.E., Bhatnagar S., 2007, ApJ, 660, L121

Irwin J., et al., 2008, ApJ, 681, 636

Ishwara-Chandra C.H., Sirothia S.K., Wadadekar Y., Pal S., Windhorst R., 2010, MNRAS, 405, 436

Johnson J.J., Jones T.J., 1991, AJ, 101, 1735

Joshi U.C., Ganesh S., Baliyan K.S., 2010, MNRAS, 402, 2744

Joshi Y.C., Narasimha D., Pandey A.K., Sagar R., 2010, A&A, 512A, 66

Kale R., Dwarakanath K.S., 2010, ApJ, 718, 939

Kato M., 1990, ApJ, 355, 277

Lyne A.G., Manchester R.N., 1988, MNRAS, 234, 477

Macario G., Venturi T., Brunetti G., Dallacasa D., Giacintucci S., Cassano R., Bardelli S., Athreya R., 2010, A&A, 517A, 43

Macario G., Markevitch M., Giacintucci S., Brunetti G., Venturi T., Murray S.S., 2011, ApJ, 728, 82 (arXiv:1010.5209)

Manoharan P.K., 2010a, in Magnetic Coupling between the Interior and Atmosphere of the Sun, Astrophysics and Space Science Proceedings, editors S.S. Hasan and R.J. Rutten, Springer, Berlin, p. 324

Manoharan P.K., 2010b, Solar Phys, 265, 137

Manoharan P.K., 2010c, Highlights of Astronomy, 15, 484

Mathew B., Subramaniam A., Bhavya B., 2010, BASI, 38, 35

Medhi B.J., Maheswar G., Brijesh K., Pandey J.C., Kumar T.S., Sagar R., 2007, MNRAS, 378, 881

Medhi B.J., Maheswar G., Pandey J.C., Tamura M., Sagar R., 2010, MNRAS, 403, 1577

Miley G., De Breuck C., 2008, A&ARv, 15, 67

Mitra D., Rankin J.M., 2011, ApJ, 727, 92 (arXiv:1011.0556)

Murgia M., Eckert D., Govoni F., Ferrari C., Pandey-Pommier M., Nevalainen J., Paltani S., 2010, A&A, 514A, 76

Naef D., et al., 2001, A&A, 375, L27

Nandi S., Pirya A., Pal S., Konar C., Saikia D.J., Singh M., 2010, MNRAS, 404, 433

Ojha D.K., Kumar M.S.N., Davis C.J., Grave J.M.C., 2010, MNRAS, 407, 1807

Paciga G., et al., 2011, MNRAS, 413, 1174 (arXiv:1006.1351)

Rankin J.M., 1993, ApJ, 405, 285

Roy J., Gupta Y., Pen Ue-Li, Peterson J.B., Kudale S., Kodilkar J., 2010, ExA, 28, 25

Roy N., Chengalur J.N., Dutta P., Bharadwaj S., 2010, MNRAS, 404, L45

Roy N., Sengupta C., Kantharia N.G., 2010, MNRAS.407, L64

Roy S., Hyman S.D., Pal S., Lazio T.J.W., Ray P.S., Kassim N.E., 2010, ApJ, 712, L5

Roychowdhury S., Chengalur J.N., Begum A., Karachentsev I.D., 2010, MNRAS, 404, L60

Saikia D.J., Jamrozy M., 2009, BASI, 37, 63

Samal M.R., et al., 2010, ApJ, 714, 1015

Serkowski K., 1965, ApJ, 141, 1340

Subramaniam A., Carraro G., Janes K.A., 2010, MNRAS, 404, 1385

Zinnecker H., Beuther H., 2008, ASPC, 387, 438